Desalination and Water Treatment
www.deswater.com

doi: 10.5004/dwt.2018.22931

124 (2018) 240–247
August

Influence of water quality on photocatalytic degradation of trace carbamazepine in real water bodies

Longli Bo*, Haixia Han, Heng Liu

School of Environmental and Municipal Engineering, Xi'an University of Architecture and Technology, Xi'an 710055, China, Tel. +86-13630232698, Fax +86-29-82202729, email: bolongli@xauat.edu.cn (L. Bo), Tel. 86-18182435035, email: 972748097@qq.com (H. Han), Tel. 86-15664671951, email: 1359016854@qq.com (H. Liu)

Received 6 February 2018; Accepted 8 August 2018

ABSTRACT

A novel $ZnIn_2S_4/TiO_2$ composite catalyst was synthesized by hydrothermal method and characterized by X-ray diffraction, UV-vis diffuse reflectance spectra and Brunauer-Emmett-Teller analysis, respectively. The photocatalytic degradation of carbamazepine (CBZ) in four actual water bodies was investigated through a batch experiment under the irradiation of an iodine-gallium lamp with the wavelength of 350~450 nm, and the effects of suspended solid (SS), inorganic salt (IS) and dissolved organic matter (DOM) on CBZ degradation were mainly discussed. Under the optimal mass ratio and dosage of $ZnIn_2S_4/TiO_2$ catalyst, the influential sequence was DOM > IS > SS for the water of Chanhe River, and IS > DOM > SS for other three water bodies from the third wastewater treatment plant of Xi'an city, China. The photocatalytic degradation of CBZ in aquatic environment followed pseudo-first-order kinetics model, and the rate constant K enhanced 2~5 times and the half-life reduced from 10~20 min to 4~5 min after the removal of SS+IS+DOM from the real water bodies.

Keywords: $ZnIn_2S_4/TiO_2$; Photocatalysis; CBZ; Influencing factor; Aquatic environment

1. Introduction

In recent years, the ecological security of aquatic environment that affected by the residue of pharmaceutical and personal care products (PPCPs) has attracted more and more attentions [1], and PPCPs exhibit adverse cumulative effects on terrestrial and aqueous ecosystems [2]. As a representative of pharmaceuticals, carbamazepine (CBZ) has been widely used to cure epileptic disease [3]. And the main discharges of medical wastewater and domestic sewage cause water pollution and bring further danger to human health due to its bioaccumulation and ecotoxicity [4]. Nowadays, CBZ was detected in waters with the concentration of μg L^{-1}~ng L^{-1} [5] and confirmed to be hardly degraded by the traditional biological processes because of its heterocyclic structure that containing nitrogen [6]. Therefore, it's necessary to study a new technology to eliminate refractory PPCPs including CBZ so as to lessen their hazards for the aquatic environment and human health.

Since 1972, Fujishima and Honda opened a prelude to heterogeneous photocatalysis [7]. Photocatalytic technology has been widely applied in the degradation of refractory pollutants, such as humic acids [8] and pharmaceutical substances [9]. With the deeper understanding of photocatalysis, single catalyst has been modified by doping [10,11] or hybrid [12], and key influence factors of photocatalytic degradation have been discussed to improve the photocatalytic efficiency. However, to the best of our knowledge, most of the researchers gave extra emphasis on the effective factors of catalyst properties, illumination intensity, substrate concentration, amount of catalyst and pH of solution etc. The effects of suspended solids (SS), dissolved organic matter (DOM) [13] and inorganic salt (IS) content in different actual water bodies on photocatalytic efficiency were rarely referred. Besides, TiO_2 has been confirmed to have high chemical stability and low cost, but its wide band gap results in mainly absorbing ultraviolet (UV) light and largely limiting the utilization of sunlight [14]. $ZnIn_2S_4$ has a narrow band gap so that it shows excellent visible light

*Corresponding author.

response and high degradation efficiency in photocatalysis of CBZ using an iodine-gallium lamp through a batch experiment [15]. However, it has disadvantages of low electron efficiency and loss of sulfur. The burgeoning composite catalyst integrates the advantages of component catalysts and exhibits higher catalytic activity and more stable structure so as to become one of research hotspots in recent decades [16]. Based on the above mentioned, $ZnIn_2S_4/TiO_2$ composite catalyst was prepared in this paper to investigate its visible light response and photocatalytic activity by characteristics and degrading experiments of CBZ in different aqueous environments, respectively. The influences of SS, DOM and IS on catalytic degradation of CBZ in four different water bodies were discussed detailedly in order to provide a scientific guide for real application of photocatalytic technology in the deep purification of natural river or the effluent from the wastewater treatment plants.

2. Material and methods

2.1. Chemicals

TiO_2 nanoparticles (P_{25} type) were purchased from Degussa Corporation of Germany. Indium nitrate ($In(NO_3)_3{\cdot}4.5H_2O$) was analytical grade and obtained from Sinopharm Chemical Reagent Co. Ltd., China. Thioacetamide (TAA) and zinc nitrate were both of analytical grade and purchased from Tianjin Kermel Chemical Reagent Co. Ltd., China. Analytically pure CBZ was supplied by Beijing J&K scientific Co. Ltd., China. In addition, HPLC-grade acetonitrile and methanol were purchased from Fisher Scientific Co., USA. All chemicals were used directly without further treatment.

Ultrapure water was obtained from PURELGA Ultra Genetic water purification system, and four real water samples were acquired from secondary sedimentation tank, rotary filter tank, disinfection tank in the third wastewater treatment plant (WWTP) of Xi'an city and Chanhe River separately. It is noted that the effluent from the third WWTP is discharged into the Chanhe River, and the sampling site of Chanhe River is in the backward of the discharged spot.

2.2. Preparation and characterization of catalyst

$ZnIn_2S_4/TiO_2$ composite catalyst was synthesized by hydrothermal method with different amounts of TiO_2 from 0.05 g to 0.2 g to optimize composite ratio. Firstly, a mixed solution was prepared by dissolving 0.4 mmol zinc nitrate, 1.0 mmol indium nitrate, a slight excess of 8.0 mmol TAA and a given amount of titanium dioxide (P_{25}) in 80 mL of ultrapure water. Then, the mixture was transferred to a 100 mL of Teflon-lined autoclave with magnetic stirring and kept at 80°C for 6 h before cooled naturally to room temperature. Next, the mixed liquor was filtrated and catalyst precursor was left onto the membrane, which was washed five times by ultrapure water to remove impure ions and dried at 80°C for 10 h. Finally, $ZnIn_2S_4/TiO_2$ composite catalyst was ground and sieved through a 325 mesh screen, and stored in a desiccator before used. As a comparison, pure $ZnIn_2S_4$ powders were prepared under similar conditions only without adding TiO_2.

The crystal phases and crystallite sizes of as-prepared catalyst were characterized by X-ray diffraction (XRD) with Cu-Kα (λ = 0.154056 nm) radiation (Ultimanlv, Germany), and the patterns were recorded 2θ ranging from 10° to 80°, at a scan rate of 10° min^{-1}. The Brunauer-Emmett-Teller (BET) specific surface area (S_{BET}) and pore structure of the catalysts were analyzed in a nitrogen adsorption-desorption apparatus (BET V-sorb 2800P, China). The sample powders were degassed at 200°C for 2 h before measured, and the S_{BET} value was calculated by multipoint BET method using adsorption data in a relative pressure (P/P_0) range of 0.05~0.3 and the pore size distribution was obtained by Barret-Joyner-Halendr (BJH) method using the data of adsorption isotherm. UV-vis diffuse reflectance spectra (DRS) were obtained on an UV-vis spectrophotometer (Babcock Hitachi U-3900, Japan) that using $BaSO_4$ as a reflectance standard.

2.3. Photocatalytic programme

Before experiment, 10 mg CBZ was weighed accurately and dissolved with ultrapure water in a 1000 mL volumetric flask to get 10 mg L^{-1} CBZ solution, which was stored in a refrigerator at 4°C. To check the influences of SS, DOM and IS on photocatalytic degradation of CBZ, raw water samples were filtered by 0.45 μm membrane filter (MF), MF and D_{301} resin (MF+D_{301}), MF and WH-18 resin (MF+WH-18), and MF+WH-18+D_{301} to remove SS, SS+DOM, SS+IS and SS+IS +DOM, respectively. A given volume of 10 mg L^{-1} CBZ solution was diluted by raw water sample or filtered water sample to 800 mL of experimental water with CBZ concentration of 100 μg L^{-1} that mainly considering the detection limit of high performance liquid chromatography (HPLC) and existing concentration of CBZ in actual water environment [17].

The photocatalytic reactor was introduced in detail in our previous work. Firstly, 800 mL of water sample containing 100 μg L^{-1} CBZ and a given amount of $ZnIn_2S_4/TiO_2$ were added to a cylindrical flask, and a quartz cold trap (ϕ60×390 mm) was inserted to keep reaction temperature constantly. Then a 100 W iodine-gallium lamp with the wavelength of 350~450 nm was settled in the centre of quartz cold trap and a magnetic stirrer was equipped at the bottom of the flask and aerated simultaneously for thorough mixing and suspension. Prior to irradiation, the mixture was firstly stirred in darkness for 30 min to achieve adsorption-desorption equilibrium for eliminating the adsorption effect. With the light on, the experiment was beginning and an aliquot of 5 mL of reactant was sampled at a given interval, then the sample was filtered through a 0.22 μm membrane to remove the catalyst and then analyzed by HPLC quantitatively.

Different water samples were applied separately to investigate the effects of SS, DOM and IS on CBZ photodegradation in experiment, and all experiments were carried out at room temperature (20±2°C) in triplicate to reduce experimental error and ensure the reproducibility.

2.4. Analytical method

CBZ concentration was quantified by HPLC with an Agilent 5 TC-C18 column (250×4.6 mm, 5 μm) and an UV detector at an excitation wavelength of 230 nm. The mobile phase containing 55% acetonitrile and 45% deionized water

was used at a constant flow rate of 0.8 mL min^{-1}. The injection volume of the sample was 100 μL and CBZ was analyzed by external standard method.

The contents of SS and IS were measured by gravimetric analysis (GB11901-89). The concentration of DOM was detected by using total organic carbon analyzer (TOC-LCPN).

3. Results and discussion

3.1. Characteristics of catalyst

The specific surface area, pore volume and pore size of TiO_2, $ZnIn_2S_4/TiO_2$ and $ZnIn_2S_4$ were calculated and listed at Table 1. The findings revealed that the specific surface area of $ZnIn_2S_4/TiO_2$ (S_{BET} = 100.98 $m^2 g^{-1}$) tended to decrease a little with the addition of TiO_2 that compared with pure $ZnIn_2S_4$, which could be due to the pore blocking of $ZnIn_2S_4$ particles by TiO_2 particles partially [18]. However, the values of specific surface area, pore volume and pore size of $ZnIn_2S_4/TiO_2$ were higher than that of TiO_2, which was beneficial to the adsorption, retention and photodegradation of pollutants on the surface of the catalyst.

XRD patterns and UV-vis DRS of $ZnIn_2S_4/TiO_2$ composite, $ZnIn_2S_4$ and TiO_2 are shown in Fig. 1. It can be seen in Fig. 1a that the diffraction peaks of $ZnIn_2S_4/TiO_2$ catalyst almost include all peaks of $ZnIn_2S_4$ and TiO_2, which indicated crystal structures of $ZnIn_2S_4$ and TiO_2 coexisted in the composite catalyst and no influences with each other. It was attributed to the hybrid formation of $ZnIn_2S_4$ on the surface of commercial TiO_2 particles, and two materials both kept their own chemical structures. The diffraction peaks of $ZnIn_2S_4$ were indexed to the hexagonal phase (JCPDS Card No. 01-072-0773) [19]. Two crystal structures of anatase and rutile were confirmed in the pristine TiO_2 while comparing with standard spectrum diagram of TiO_2 (PDF-#21-1272 TiO_2-Anatase, PDF-#21-1276 TiO_2-Rutile), which was consistent with a relevant report [20].

Table 1
The surface properties of different catalysts

Catalysts	Specific surface area ($m^2 g^{-1}$)	Pore volume ($cm^3 g^{-1}$)	Pore size (nm)
TiO_2	8.569	0.332	56.77
$ZnIn_2S_4/TiO_2$	100.98	2.110	59.83
$ZnIn_2S_4$	118.34	1.341	45.52

The crystallite size (D) is calculated using Scherrer's formula [21].

$$D = \frac{0.89\lambda}{\beta COS(\theta)} \quad (1)$$

where λ, θ and β are the X-ray wavelength, Bragg diffraction angle and the experimental full-width at half-maximum. According to the calculation, the crystalline sizes of $ZnIn_2S_4$ and $ZnIn_2S_4/TiO_2$ were to be 2.89 nm and 4.06 nm, respectively. The envelope of yellow $ZnIn_2S_4$ onto TiO_2 induced to form bigger hybrid crystals.

Fig. 1b shows that $ZnIn_2S_4/TiO_2$ composite and pure $ZnIn_2S_4$ both had strong absorption from UV to visible light with an absorption edge at about 620 nm, and TiO_2 only had an absorption ability in UV region. $ZnIn_2S_4/TiO_2$ had a little stronger absorption than pure $ZnIn_2S_4$ below 500 nm that including the response wavelength of iodine-gallium light (350~450 nm) due to the existence of TiO_2. The band gaps of $ZnIn_2S_4/TiO_2$, $ZnIn_2S_4$ and TiO_2 were determined to be 1.9 eV, 1.89 eV and 3.0 eV separately by the intersection of two extrapolated straight lines from the plots of $(\alpha h\nu)^{1/2}$ versus $h\nu$ (insert of Fig. 1b), consistent with the previous reports [22,23]. It indicated that $ZnIn_2S_4/TiO_2$ can effectively absorb UV and visible light in this work, and hybrid TiO_2 had little effect on its light-absorbing property while comparing with $ZnIn_2S_4$.

3.2. Optimization of catalyst component and dosage

To have a good photocatalytic degradation, it is necessary to optimize catalyst component and dosage. There-

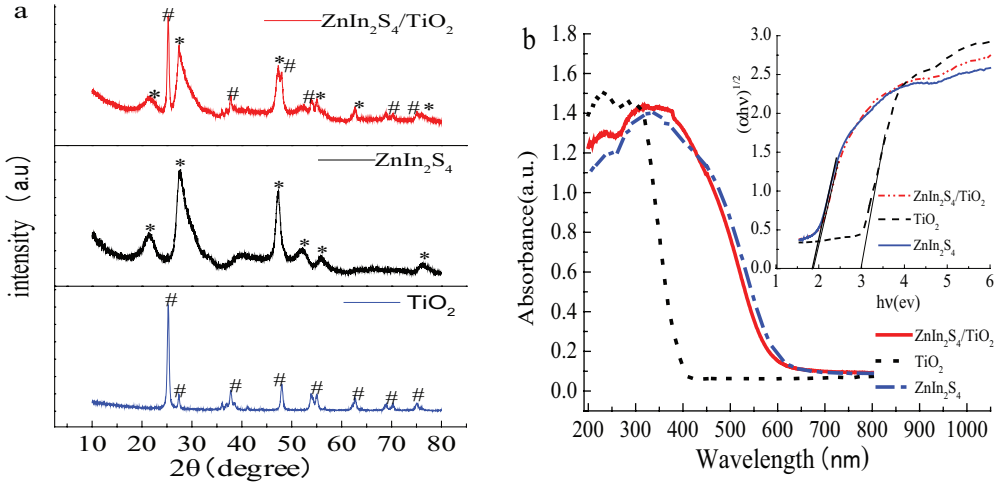

Fig. 1. Different characteristics of the catalysts. (a) XRD patterns of $ZnIn_2S_4/TiO_2$, $ZnIn_2S_4$ and TiO_2. (b) UV-vis diffuse reflectance spectra. Insert, plots of $(\alpha h\nu)^{1/2}$ vs. $h\nu$.

fore, 800 mL of water sample from rotary filter tank was taken as the target and CBZ was added to be 100 μg L^{-1}, and $ZnIn_2S_4$ amount, mass ratio of $ZnIn_2S_4$ to TiO_2 and dosage of $ZnIn_2S_4/TiO_2$ were gradually optimized by a series of experiments and the results are presented in Fig. 2.

Fig. 2a shows the photocatalytic degradation of CBZ by different amounts of $ZnIn_2S_4$ and direct photolysis of CBZ without the addition of $ZnIn_2S_4$. It indicated that CBZ could be completely transformed by direct photolysis and the best dosage of $ZnIn_2S_4$ was 112.5 mg L^{-1} in experiment. Photolysis of CBZ had been confirmed in our previous work, which could be mainly due to an irradiation wavelength of 350~450 nm that including both UV and visible light. $ZnIn_2S_4$ can produce active species to speed up the reaction under irradiation, but more $ZnIn_2S_4$ also reduce light transmittance due to light reflection of metal particles and penetration depth of light [24].

Under total amounts of 112.5 mg L^{-1}, mass ratios of $ZnIn_2S_4$ to TiO_2 were checked at 17/5, 17/10, 17/15 and 17/20, respectively. It can be seen in Fig. 2b that less amounts of TiO_2 improved the degradation of CBZ, but more TiO_2 decreased the catalytic activity comparing with pure $ZnIn_2S_4$. It pointed out that $ZnIn_2S_4$ was the main catalyst and a small amount of TiO_2 could promote the separation of photo-generated electron-hole (e^--h^+) pairs and simultaneously accelerate the transfer of photo-generated carriers [25]. Fixed the optimal mass ratio of 17/10, the optimal dosage of $ZnIn_2S_4/TiO_2$ catalyst was verified to be 75 mg L^{-1} in Fig. 2c, which exhibited high degradation efficiency and little influence dosage of $ZnIn_2S_4/TiO_2$ in photocatalysis of CBZ.

3.3. Affecting analysis of different water quality parameters

Under the optimal mass ratio and dosage of $ZnIn_2S_4/TiO_2$ catalyst, four raw water samples were separately taken as the matrix to check the influences of SS, DOM and IS in photocatalytic degradation of CBZ. Relative water quality parameters of four water bodies and experimental results of photocatalysis are shown in Table 2 and Fig. 3, respectively.

It can be seen in Table 2 that four water samples all had a high salt content and a relatively low TOC value, which indicated large amounts of IS and less DOM exist in water bodies. The SS values in the water sample of the Chanhe River are higher than that of the other three samples. MF can remove SS completely, which also has a less removal for TOC and salt content due to the adsorption of SS to DOM and IS. WH-18 resin can reduce salt content of the samples very effectively due to a strong adsorption to IS, and also decrease TOC in some degree due to the adsorption of resin and IS to organic substances. D_{301} resin has a strong removal

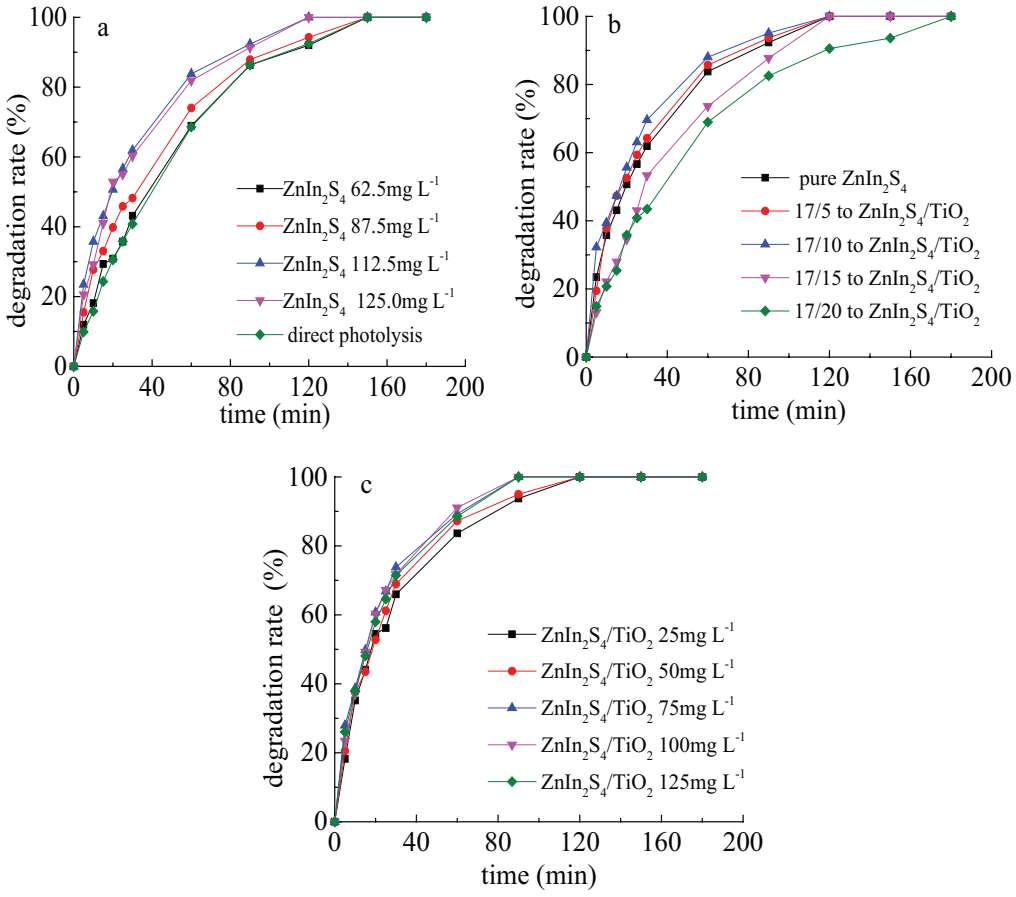

Fig. 2. Optimizing experiments of the catalysts. (a) The optimization of $ZnIn_2S_4$ amount. (b) The optimal mass ratio of $ZnIn_2S_4$ to TiO_2. (c) The optimal dosage of $ZnIn_2S_4/TiO_2$.

Table 2
Relative water quality parameters of four water samples

Sample	Process method	mg L^{-1}		
		SS	TOC	Salt content
Chanhe River	Raw water	73	20.27	792
	MF	0	19.35	695
	MF+WH-18	0	14.12	92
	MF+D_{301}	0	2.080	627
	MF+WH-18+D_{301}	0	1.372	74
Rotary filter tank	Raw water	15	16.77	876
	MF	0	15.20	813
	MF+WH-18	0	13.45	131
	MF+D_{301}	0	2.298	798
	MF+WH-18+D_{301}	0	1.102	101
Disinfection tank	Raw water	17	18.21	853
	MF	0	17.81	790
	MF+WH-18	0	13.12	121
	MF+D_{301}	0	1.609	672
	MF+WH-18+D_{301}	0	1.120	100
Secondary sedimentation tank	Raw water	34	18.36	791
	MF	0	17.18	700
	MF+WH-18	0	16.39	82
	MF+D_{301}	0	1.317	610
	MF+WH-18+D_{301}	0	0.989	56

ability for DOM, causing TOC to drop, meanwhile, the resin also has a certain removal efficiency for inorganic salt. Therefore, the process methods listed in Table 2 can effectively remove SS, DOM and IS from the matrix to provide necessary water samples for analyzing their effects on photocatalytic degradation of CBZ.

It is shown in Fig. 3 that CBZ in four water bodies treated with different processes could be completely degraded within 60 min or 90 min. CBZ in the water sample of Chanhe River had a faster photodegradation rate than other three samples from the WWTP, and the removals of SS, SS+IS, SS+DOM and SS+IS +DOM from four water samples all had positive effects on the photocatalysis of CBZ. It also can be seen in Fig. 3b, 3c and 3d that similar trends appeared to three water samples from disinfection tank, rotary filter tank and secondary sedimentation tank, and the effects of SS, IS and DOM on photodegradation of CBZ in these three samples were more distinguished than in that of Chanhe River. It had been confirmed in our previous work that the photocatalytic degradation of CBZ in aquatic environment followed pseudo-first-order kinetics model. Therefore, reaction kinetics was investigated in order to further quantify the influences of SS, IS and DOM on the removal of CBZ, and the fitted curves and relatively analytical data are given in Fig. 4 and Table 3, respectively.

It is clearly seen in Fig. 4 that the fitted curves of CBZ photodegradation in raw water samples and other treated water samples were in accordance with the first-order kinetics model and correlation coefficients (R^2, seen in Table 3) were all higher than 0.9. It was verified once again

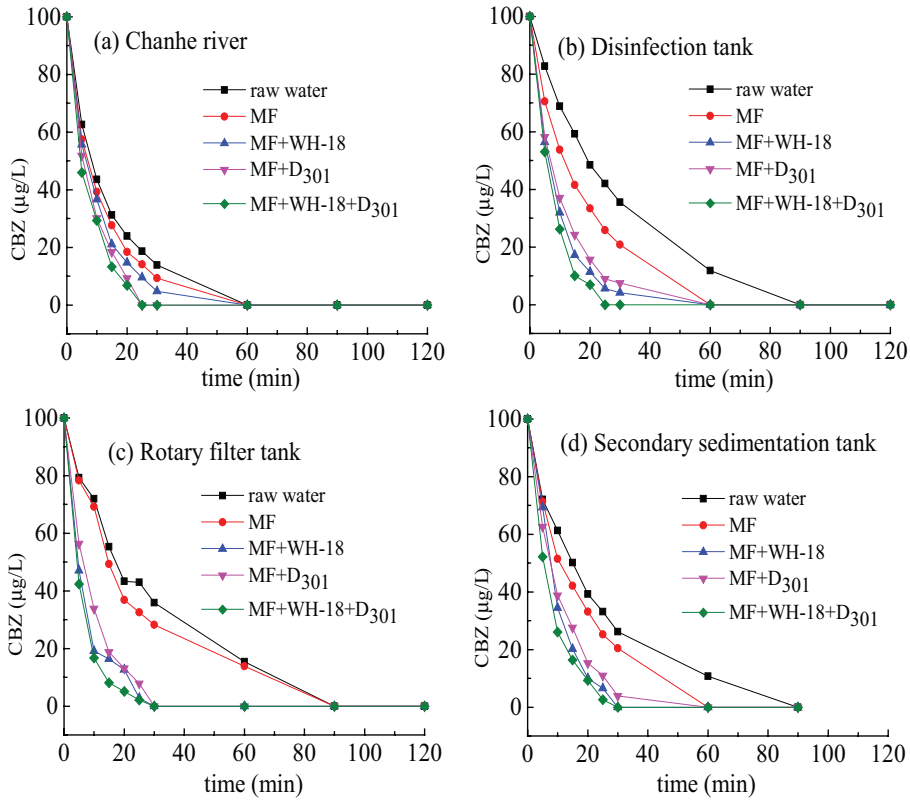

Fig. 3. The photocatalytic degradation of CBZ in four raw water samples and other samples that treated by different processes.

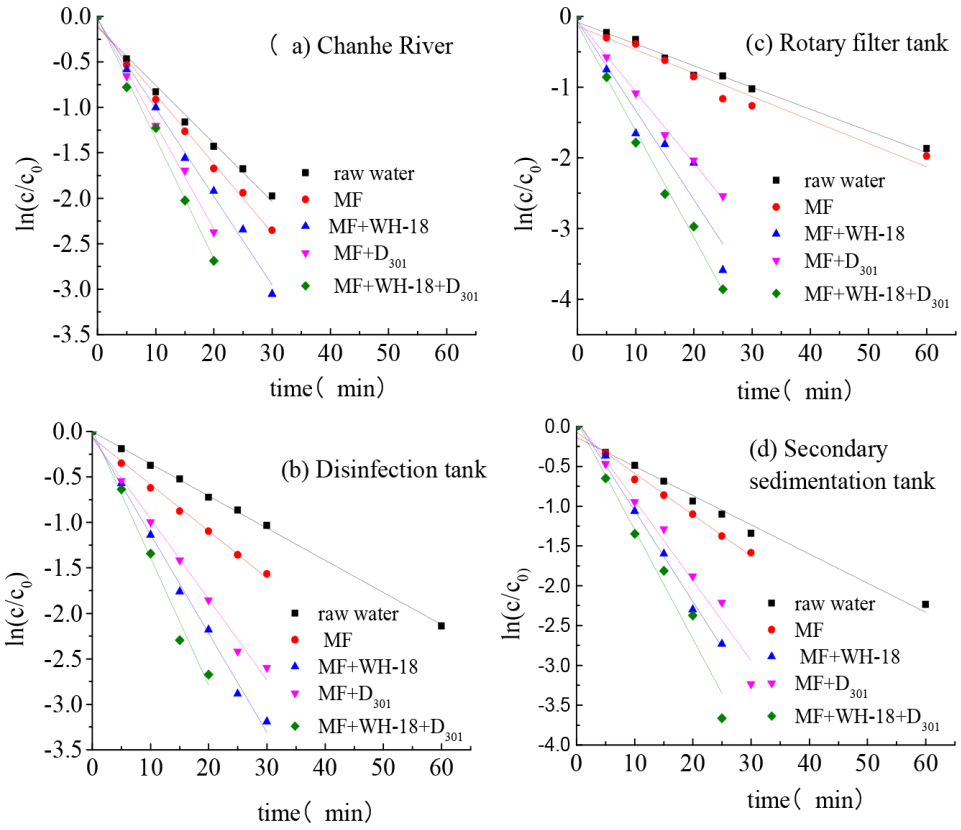

Fig. 4. Reaction kinetics of CBZ photodegradation in different water samples.

Table 3
Relevant parameters of reaction kinetics for the photodegradation of CBZ

Parameter	Process method	Chanhe River	Rotary filter tank	Disinfection tank	Secondary sedimentation tank
Rate constant (k) / min^{-1}	Raw water	0.0639	0.0307	0.0307	0.0307
	MF	0.0760	0.0331	0.0333	0.0331
	MF+WH-18	0.0971	0.1259	0.1259	0.1259
	$MF+D_{301}$	0.1157	0.1010	0.1010	0.1008
	$MF+WH-18+D_{301}$	0.1324	0.1506	0.1506	0.1506
Half-life ($t_{1/2}$) / min	Raw water	10.85	22.58	22.58	22.58
	MF	9.12	20.94	20.81	20.94
	MF+WH-18	7.14	12.53	5.51	5.51
	$MF+D_{301}$	5.99	6.86	6.86	6.88
	$MF+WH-18+D_{301}$	5.24	4.60	4.60	4.60
Correlation coefficient (R^2)	Raw water	0.9859	0.9823	0.9823	0.9823
	MF	0.9932	0.9551	0.9433	0.9551
	MF+WH-18	0.9931	0.9100	0.9100	0.9096
	$MF+D_{301}$	0.9963	0.9950	0.9949	0.9950
	$MF+WH-18+D_{301}$	0.9928	0.9895	0.9895	0.9895

that the photocatalytic degradation of CBZ in aqueous environment followed pseudo-first-order reaction kinetics, and the photodegradation rate of CBZ increased gradually with the removals of SS, SS+IS, SS+DOM and SS+IS +DOM, respectively.

The rate constants of CBZ photodegradation in four raw water samples and treated water samples without SS, SS+IS, SS+DOM and SS+IS +DOM separately are given in Table 3. The independent influences of SS, IS and DOM on the photocatalysis of CBZ could be calculated by a deviation

between "raw water" and "MF", "MF" and "MF+WH-18" and "MF" and "MF+D_{301}". For the water sample of Chanhe River, the individual influences of SS, IS and DOM on rate constant K were 0.0121 min^{-1}, 0.0211 min^{-1} and 0.0397 min^{-1} respectively, so the influential degree was DOM > IS > SS. Compared "raw water" with "MF+WH-18+D_{301}", the rate constant K increased more than 2 times and the half-life reduced from 10.85 min to 5.24 min, which demonstrated that the removal of SS+IS+DOM from water body could effectively improve the degradation rate of CBZ and greatly shorten the degradation time. For other three samples from rotary filter tank, disinfection tank and secondary sedimentation tank, there were same trends for the influences of SS, IS and DOM on CBZ degradation, and the influential sequences were all IS > DOM > SS. The rate constant K enhanced nearly 5 times and the half-life shortened from 22.58 min to 4.60 min after the removal of SS+IS+DOM from three raw water samples.

The influence of SS on the photocatalytic degradation of CBZ was mainly attributed to two sides. For one side, SS can increase the turbidity of water to reduce the photopermeability that lead to block the connection between the catalyst and light and further inhibit the photocatalytic reaction [26]. For the other side, SS has a certain adsorption on the ions in the water, which affects CBZ adsorption on the surface of $ZnIn_2S_4/TiO_2$ and the dispersion of the catalyst. Generally, it's a combined result of both two sides to decrease the catalytic activity [27].

After the treatment of WH-18 resin, IS could be mostly removed from water samples (Table 2). It is seen in Fig. 4 and Table 3, comparing with the water from Chanhe River, IS played a more important role in the photodegradation of CBZ in three water bodies from the WWTP. Based on the analysis of water quality, it proved that the water of Chanhe River mainly included nitrate ion, chloride ion, calcium and magnesium cation etc, and other three waters from the WWTP primarily contained chloride ion, sulfate, hypochlorite and sodion etc. It was reported that low concentration of nitrate (less than 10^{-4} mol L^{-1}) could accelerate the photocatalytic degradation of contaminants, and also had the competitive adsorption or reacted with the hole and hydroxyl radical so as to inhibit the photodegradation of contaminants with the increasing of concentration [28]. However, sulfate and chloride ions could inhibit photocatalysis as a result of both of them would react with hole and electron and simultaneously exist competitive adsorption [29]. And it's worth noting that the inhibition of sulfate is stronger than chloride because sulfate ion has more charges than chloride ion. Sodium, magnesium, calcium and other cations have no obvious effects on the photocatalytic rate during the oxidative reaction. Therefore, the different influences of IS in the photocatalysis of CBZ in actual water bodies between Chanhe River and the WWTP could be attributed to the different component and content of various anions. The higher ion concentration, the stronger inhibitory effect on photocatalysis.

Additionally, DOM also had an obvious effect on the photodegradation of CBZ, especially for the water of Chanhe River, which owned a little higher TOC value than those of the WWTP (Table 2). The research had been found that the photocatalytic efficiency was related to the amounts of DOM in aqueous solution [30], which mainly affected photocatalytic degradation in the following aspects. Firstly, it has a strong capacity to absorb light, especially for UV-light, and competes photo-generated electron with CBZ to weaken the useful light intensity in reaction. Secondly, DOM could compete the active sites with CBZ to inhibit its photocatalysis. It has been reported that the composite of electron and hole on the surface of catalyst can be finished at less than 10^{-9} s, while the capture rate of the carrier is usually 10^{-8}~10^{-7} s, which states that only the adsorbed pollutants on the catalyst surface may be degraded. Under a given surface area, the decrease of activity sites can apparently reduce the reaction rate [31]. Furthermore, some substances of DOM can capture the holes and hydroxyl radicals on the surface catalyst. Finally, CBZ itself also has a good combination with DOM compounds [32].

4. Conclusions

The research work in this study clearly indicated that trace CBZ in real water bodies could be completely degraded by photocatalysis as quickly as possible within 30 min, 60 min or 90 min. TiO_2 was enveloped by yellow $ZnIn_2S_4$ to exhibit larger pore size and stronger photoabsorption ability under irradiation of iodine-gallium light that was beneficial to the degradation of CBZ on the surface of $ZnIn_2S_4/TiO_2$. The optimal mass ratio and dosage were 17/10 and 75 mg/L respectively to $ZnIn_2S_4/TiO_2$ catalyst in experiment, and less hybrid TiO_2 was speculated to effectively promote the separation of e^--h^+ pairs and accelerate the transfer of photo-generated carriers simultaneously. Water quality parameters, such as SS, IS and DOM, had apparently negative influences on photodegradation of CBZ. SS reduced the photopermeability and CBZ adsorption on the catalyst surface. Sulfate and chloride ions existing in the water samples can react with hole and electron and also can be absorbed on the surface of the catalyst to inhibit the photocatalytic reaction. The competition of DOM with CBZ can weaken the degradation of CBZ from the aspects of light intensity, active sites, free radicals and adsorption etc. Therefore, the removal of SS, IS and DOM in real water bodies can improve the photocatalytic degradation of CBZ effectively.

Acknowledgments

This work was supported by the key technological innovation team of Shaanxi Province (2017KCT-19-01) and the innovative research team of Xi'an University of Architecture and Technology.

References

[1] M. Saghi, K. Mahanpoor, Photocatalytic degradation of tetracycline aqueous solutions by nanospherical α-Fe_2O_3 supported on 12-tungstosilcis acid as catalyst: using full factorial experimental design, Int. J. Ind. Chem., 8 (2017) 297–313.

[2] Y. Yang, Y.S. Ok, K.H. Kim, E.E. Kwon, Y.F. Tsang, Occurrences and removal of pharmaceuticals and personal care products (PPCPs) in drinking water and water/sewage treatment plants: A review, Sci. Total Environ., 596–597 (2017) 303–320.

[3] S.I. Natali, D. Fumagalli, Fast photocatalytic degradation of pharmaceutical micropollutants and ecotoxicological effects, Environ. Sci. Pollut. Res., 24 (2016) 1–6.
[4] B. Czech, W. Cwikla-Bundyra, Advanced oxidation processes in Triton X-100 and wash-up liquid removal from wastewater using modified TiO_2/Al_2O_3 photocatalysts, Water Air Pollut., 223 (2012) 4813–4822.
[5] M. Farzadkia, E. Bazrafshan, A. Esrafili, J.K. Yang, M. Shirzad-siboni, Photocatalytic degradation of metronidazole with illuminated TiO_2 nanoparticles, J. Environ. Health Sci. Eng., 13 (2015)1–8.
[6] L.L. Bo, K.B. He, N. Tan, B. Gao, Q.Q. Feng, J.D. Liu, L. Wang, Photocatalytic oxidation of trace carbamazepine in aqueous solution by visible-light-driven $ZnIn_2S_4$: Performance and mechanism, J. Environ Manage., 190 (2017) 259–265.
[7] A. Fujishima, K. Honda, Electrochemical photolysis of water at a semiconductor electrode, Nature, 238 (1972) 37–38.
[8] C.Y.P. Ayekoehia, D. Robert, D.G. Lanciné, Combination of coagulation-flocculation and heterogeneous photocatalysis for improving the removal of humic substances in real treated water from Agbô River (lvory-Coast), Catal. Today, 281 (2017) 2–13.
[9] S.K. Alharbi, W.E. Price, J.G. Kang, T. Fujioka, L.D. Nghiem, Ozonation of carbamazepine, diclofenac, sulfamethoxazole and trimethoprim and formation of major oxidation products, Desal. Water Treat., 57 (2016) 29340–29351.
[10] J.F. Guo, Y.Y Li, D. Hu, H. Liu, Preparation of transition-metal-doped ZnO nanophotocatalysts and their performance on photocatalytic degradation of antibiotic wastewater, Desal. Water Treat., (2014) 1–8.
[11] A.T. Kuvarega, B.B. Mamba, TiO_2-based photocatalysis: toward visible light-responsive photocatalysts through doping and fabrication of carbon-based nanocomposites, Crit. Rev. Solid State Mater. Sci., 42 (2017) 295–346.
[12] S. Dominguez, M. Huebra, C. Han, P. Campo, M.N. Nadaqouda, M.J. Rivero, I. Oritiz, D.D. Dionysiou, Magnetically recoverable TiO_2-WO_3 photocatalyst oxidize bisphenol A from model wastewater under simulated solar light, Environ. Sci. Pollut. Res., 24 (2017) 12589–12598.
[13] S.K. Maeng, K. Cho, B. Jeong, J. Lee, Y. Lee, C. Lee, K.J. Choi, S.W. Hong, Substrate-immobilized electrospun TiO_2 nanofibers for photocatalytic degradation of pharmaceuticals: The effects of pH and dissolved organic matter characteristics, Water Res., 86 (2015) 25–34.
[14] A. Bojanowska-Czajka, G. Kciuk, M. Gumiela, B. Borowiecka G. Nateczjawecki, A. Koc, J.F. Garcia-Reyes, D. Solpan Ozbay, M. Trojanowicz, Analytical, toxicological and kinetic investigation of decomposition of the drug diclofenac in waters and wastes using gamma radiation, Environ. Sci. Pollut. Res., 22 (2015) 20255–20270.
[15] L.L. Bo, T. Urase, X.C. Wang, Biodegradation of trace pharmaceutical substances in wastewater by a membrane bioreactor, Front Environ. Sci. Eng. in China, 3 (2009) 236–240.
[16] Y. Xia, Q. Li, K.L. Lv, M. Li, Heterojunction construction between TiO_2 hollowsphere and $Znln_2S_4$ flower for photocatalysis application, Appl. Surf. Sci., 398 (2017) 81–88.
[17] S. González Alonson, M. Catalá, R. Romo Maroto, J.L. Rodíguez Gil, D.M.Á. Gil, Y. Valcárcel, Pollution by psychoactive pharmaceuticals in the rivers of Madrid metropolitan area (Spain), Environ. Int., 36 (2010) 195–201.
[18] O. Rojviroon, T. Rojviroon, S. Sirivithayapakorn, Removal of color and chemical oxygen demand from landfill leachate by photocatalytic process with AC/TiO_2, Energy Procedia., 79 (2015) 536–541.
[19] Y.X. Li, J.X. Wang, S.Q. Peng, G.X. Lu, S.B. Li, Photocatalytic hydrogen generation in the presence of glucose over ZnS-coated $ZnIn_2S_4$ under visible light irradiation, Int. J. Hydrogen Energy, 35 (2010) 7116–7126.
[20] W.P. Chen, Y. Wang, Z.S. Jin, C.X. Feng, Z.S. Wu, Z.J. Zhang, Influence of NH_3-treating temperature on visible light photocatalytic activity of N-doped P25-TiO_2, Sci. China Ser B-Chem., 52 (2009) 1164–1170.
[21] A. Jrad, T.B. Nasr, N. Turki-kamoun, Study of structural,optical and photoluminescence properties of indium-doped zinc sulfide thin films for photoelectronic applications, Opt. Mater., 50 (2015) 128–133.
[22] B. Chai, T.Y. Peng, P. Zeng, X.H. Zhang, X.J. Liu, Template-free hydrothermal synthesis of $ZnIn_2S_4$ floriated microsphere as an efficient photocatalyst for H_2 production under visible-light irradiation, J. Phys. Chem. C., 115 (2011) 6149–6155.
[23] H. Yin, Y. Wada, T. Kitamura, S. Kambe, S. Murasawa, Hydrothermal synthesis of nanosized anatase and rutile TiO_2 using amorphous phase TiO_2, J. Mater. Chem., 11 (2001) 1694–1703.
[24] W. Chen, L. Zhao, H. Xu, J. Yang, Photocatalytic degradation characteristics of carbamazepine over activated carbon supported TiO_2, J. Civ. Archit. Environ. Eng., 34 (2012) 126–131.
[25] B.F. Abramović, V.N. Despotović, D.V. Šojić, D.Z. Orčić, J.J. Csanádi, D.D. Četojević-Simin, Photocatalytic degradation of the herbicide clomazone in natural water using TiO_2: Kinetics, mechanism, and toxicity of degradation products, Chemosphere, 93 (2013) 166–171.
[26] H. Woo, J. Park, J. Kim, S. Park, H.P. Kang, Hierarchical hybrid MnO/Pd-Fe_3O_4 and CoO/Pd-Fe_3O_4 nancomposites as efficient catalysts for hydroboration of styrene, Catal. Commun., 100 (2017) 52–56.
[27] E. Regulska, D.M. Brus, P. Rodziewicz, S. Sawicka, J. Karpinska, Photocatalytic degradation of hazardous Food Yellow 13 in TiO_2 and ZnO aqueous and river water suspensions, Catal. Today, 266 (2016) 72–81.
[28] C.J. Escudero, O. Iglesias, S. Dominguez, M.J. Rivero, I. Ortiz, Performance of electrochemical oxidation and photocatalysis in terms of kinetics and energy consumption, New insights into the p-cresol degradation, J. Environ. Manage., 195 (2017) 117–124.
[29] A.M. Dugandžić, A.V. Tomašević, M.M. Radišić, N.Ž. Šekuljica, D.Ž. Mijin, S.D. Petrović, Effect of inorganic ions, photosensitisers and scavengers on the photocatalytic degradation of nicosulfuron, J. photochem. photobiol. A: Chem., 336 (2017) 146–155.
[30] J. Park, H.L. Nam, J.W. Choi, J. Ha, S.H. Lee, Oxidation of geosmin and 2-methylisoborneol by the photo-fenton process: kinetics, degradation intermediates, and the removal of microcystin-LR and trihalomethane from Nak-Dong River Water, South Korea, Chem. Eng. J., 313 (2017) 345–354.
[31] Q.Q. Zhao, J. Sun, J.B. Li, J.X. He, Kinetics and mechanism of Horner-Wadsworth-Emmons reaction of weakly acidic phosphonate in solid-liquid phase-transfer catalysis system, Catal. Commun., 36 (2013) 98–103.
[32] Y.Y. Sun, Y. Wang, N. Xue, C. Yu, Y.J. Meng, B.Y. Gao, Q.L. Li, The effect of DOM on floc formation and membrane fouling in coagulation/ultrafiltration process for treating TiO_2 nanopartiicles in various aquatic media, Chem. Eng. J., 316 (2017) 429–437.